The Journal of Phytopharmacology 2023; 12(3):152-163
Online at: www.phytopharmajournal.com

Research Article

ISSN 2320-480X
JPHYTO 2023; 12(3): 152-163
May- June
Received: 09-04-2023
Accepted: 01-06-2023
Published: 30-06-2023

doi: 10.31254/phyto.2023.12303

Veerabhuvaneshwari Veerichetty
Department of Biotechnology, Kumaraguru College of Technology Coimbatore, Tamil Nadu, India

Iswaryalakshmi Saravanabavan
Department of Biotechnology, Kumaraguru College of Technology Coimbatore, Tamil Nadu, India

Abiraamasundari Ramapalaniappan
Spinos Life science and Research Private Limited

Correspondence:
Veerabhuvaneshwari Veerichetty
Department of Biotechnology, Kumaraguru College of Technology Coimbatore, Tamil Nadu, India
Email:
veerabhuvaneshwari.v.bt@kct.ac.in

In silico kinase inhibition profiling of BRAF and AKT Signaling in Melanoma Cells with Nuciferine

Veerabhuvaneshwari Veerichetty, Iswaryalakshmi Saravanabavan, Abiraamasundari Ramapalaniappan

ABSTRACT

The RAS/RAF and PI3K/AKT pathways play a crucial regulatory role and oncogenic mutation of key proteins in these pathways leads to cancer metastasis and chemoresistance. Melanoma is triggered by NRAS and BRAF V600E mutation which causes constitutive activation of the PI3K kinase and BRAF kinase respectively, further leading to oncogenic activation of the AKT kinase and mitogen-activated protein kinase (MAPK). Core regulatory network behind MAPK and AKT cascades interconnect and form feedback loops. This crosstalk between the two pathways plays a vital role in melanoma kinase inhibitor resistance. Nuciferine is found in the plants *Nelumbo Nucifera* and *Nymphaea Caerulea.* Nuciferine is the main aporphine alkaloid produced in *Nelumbo nucifera*. Nuciferine have the best efficiency to remove oxygen free radicals and hydroxyl free radicals. Nuciferine have potent ROS scavenging activity. Nuciferine provokes anti-inflammation, anti-psychotic drug, anti-cancer treatment, and anti-obesity diseases. This in silico analysis results reinforces nuciferine has an effective kinase inhibitor with a potential advantage of evading resistance in melanoma by dual targeting. The residues of the substrate binding pockets were identified using literature search. Molecular docking studies was carried out using AutoDock. Docking studies indicated nuciferine and vemurafenib (reference standard) showed better binding affinity for kinase pockets of Braf V600E, MEK, ERK, PI3K, AKT, mTOR and c-KIT. -7.00Kcal/mol is considered as the cut-off energy for inhibition analysis. Hydrophobic interactions were computed using Biovia. Biovia was used for the graphical representation of protein ligand binding.

Keywords: BRAF, AKT, Kinase inhibitors, Docking, Nuciferine, Vemurafenib, Melanoma.

INTRODUCTION

Nuciferine is an aporphine alkaloids, which is isolated from *Nelumbo Nucifera Gaertn* (pink lotus). Nuciferine deals with dopamine receptor blockade. Alkaloids, which are thought to be the main bioactive components of the plant, are abundant in the leaf, according to phytochemical investigations. In lotus leaf, it is very rich in Nuciferine, that contains high content of aporphine alkaloid. Nuciferine is the excellent source for anti-cancer and anti-inflammation. It has also other uses such as lowering blood sugar levels, diarrhea and cholera. Nuciferine is also used as anti-psychotic drugs. It is used for removing toxicity from skin and it gives moisture to skin also.

One of the malignancies with the most mutation is melanoma. Transmembrane tyrosine kinase (c-KIT) is a promising target in melanoma. NRAS is an aggressive oncogene, Neuroblastoma RAS that is manipulated to 30% of melanoma. RAS pathway that activates dual cascades that is RAS-ERK pathway and PI3K-AKT pathway. BRAF is among the most common frequently occurring oncogenic skin cancer. The most typical BRAF variant is glutamic acid swapping for valine (BRAF V600E). Maximum number of people (40%-50%) with skin cancer is due to the BRAF V600E mutation [1]. At the early discovery of Sorafenib was a failure to BRAF mutation pathway to be inhibited. So, recently discovered that Vemurafenib has high potential to inhibit BRAF pathway. A greater advancement in patient care in terms of response rates and overall survival was improved by using a fusion of BRAF inhibitors and BRAF cascade kinases (MAP2K 1/2) mitogen-activated protein kinase kinases [2]. RAS that binds with PI3K and activates AKT pathway, PIP3 is a subordinate messenger that binds with PI3K and activates AKT cascade. mTOR is the important downstream of PI3K-AKT pathway [3]. mTOR function is to inhibit autophagocytosis. Phosphorylation of AKT results in reduced caspase activation and enhanced melanoma survival. Mutations in KIT were more common in epithelium, Acral lentiginous melanoma, and horrendously sun-damaged skin melanoma than in non-chronic sun damaged skin melanoma. RTK are mainly involved in tumors of epithelial origin and melanoma. Embodies RAS-ERK pathway and PI3K-AKT pathway (Figure 1) [4].

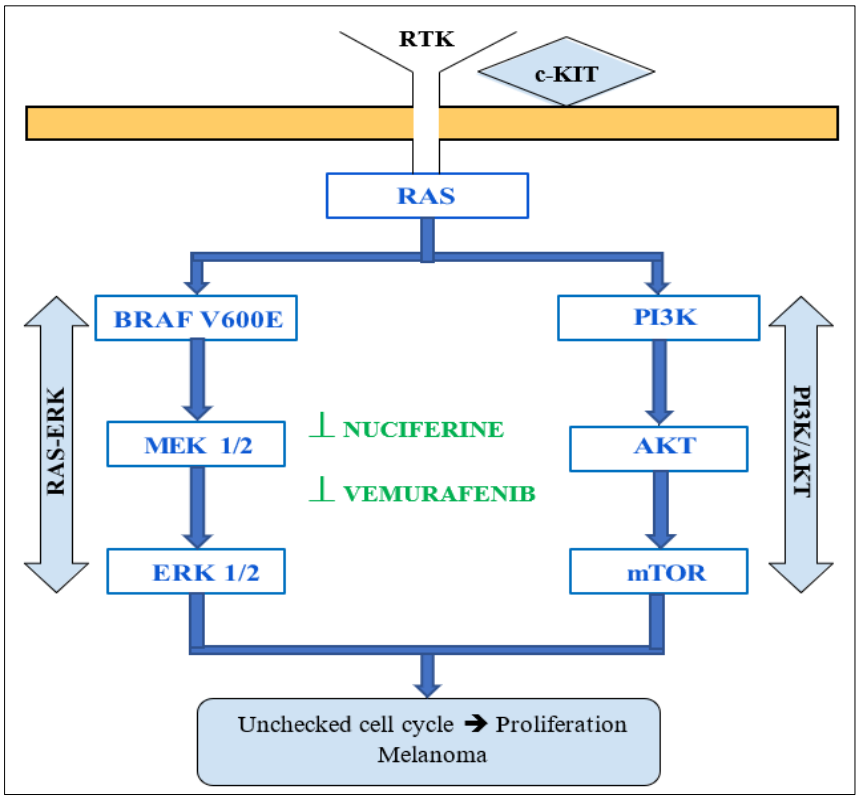

Figure 1: Illustration OF RAS-ERK pathway and PI3K-AKT pathway

MATERIALS AND METHODS

Target Selection of Protein

The RAC-Alpha Serine/Threonine-Protein Kinase (AKT-1) protein sequence (PDB ID : 3O96), B-Raf V600E Kinase (BRAF V600E) protein sequence (PDB ID : 3OG7) and Extracellular Signal-Regulated Kinases -2 (ERK-2) protein sequence (PDB ID : 3I60) proteins are taken [5, 6, 7]. Mammalian Target Of Rapamycin (mTOR) protein sequence (PDB ID: 4JSX), Phosphatidylinositol-3-Kinase (PI3K) protein sequence (PDB ID : 4WAF), Mitogen-Activated Protein Kinase Kinase -1 (MEK-1) protein sequence (PDB ID : 3SLS) proteins are taken [8, 9, 10]. Receptor Tyrosine Kinase (c-Kit) protein sequence (PDB ID : 3G0E) are the proteins that are retrieved from Protein Data Bank (PDB) [11, 12].

Ligand Preparation

The ligands were taken in Pub-Chem, (Nuciferine: PubChem CID – 10146) and reference drug Vemurafenib PubChem CID – 42611257 [13, 14]. The residues forming the binding pockets, kinase was identified based on extensive literature search.

In Silico Biological Activity and Admet Analysis

Pharmacodynamics Biological activity prediction of the compunds using the PASS-Way2Drug server (http://www.way2drug.com/PASSOnline/) [15]. SwissADME and PreADMET (https://preadmet.qsarhub.com/) web tool was used to predict the pharmacokinetic parameters of Nuciferine and Vemurafenib [16 , 17, 18].

In Silico Kinase Inhibition Profiling of Nuciferine

BRAF is major type of mutant for skin melanoma. This belongs to kinase family. RAS triggers two mutation paths, that leads to melanoma. RAS-ERK and PI3K-AKT are two different paths which downstream to proliferation and melanoma (Table 1). BRAF is a serine/threonine kinase that functions directly before MAP2K1/2, also known as mitogen-activated extracellular signal-regulated kinases 1/2 (MEK1/2), which subsequently trigger ERK1/2. *In silico* studies were done, using Nuciferine and Vemurafenib (standard drug). Autodock Vina 4.2 was used for molecular docking. BIOVIA Discovery Studio Visualizer was used for pictorial representation for protein-ligand binding and also used for analyzing hydrogen interactions.

Optimization of Binding Affinity and Inhibition Constant

Using Auto Dock Vina 1.5.6, the binding affinity of the protein-ligand complex was determined [19, 20]. Whereby heteroatoms initially eliminated, followed by the addition of hydrogen bonds and Gasteiger charges. Using AutoGrid v.4.2, the grid box dimension was fixed at a 40x40x40 A˚ with a spacing of 0.375 A˚. Relationship between binding energy and Inhibition constant (Ki) of Nuciferine and Vemurafenib was calculated using, Ki = exp(ΔG/RT), where R is the universal gas constant (1.985 × 10^{-3} kcal mol−1 K−1) and T is the temperature (298.15 K) [21].

RESULTS AND DISCUSSION

AutoDock Vina 1.5.6 is used for docking and binding energies, hydrogen bond interactions were calculated. Nuciferine was compared with Vemurafenib (as reference drug). Vemurafenib is used for standard drug for targeting of skin melanoma treatment, especially BRAF proteins they are targeting for inhibition for further process [22]. Nuciferine exhibits anticancer action via inducing oxidative stress, preventing the progression of cells, and a number of other mechanisms. Contrasting to antitumor medications, it offers a variety

of therapeutic uses, including anti-inflammatory, anti-anxiety, and anti-cancerous.

In Silico Kinase Inhibition Profiling

Ligand and Protein Retrieval and Preparation

The following Retrieval of proteins from Protein Data Bank are RAC-Alpha Serine/Threonine-Protein Kinase (AKT-1) PDB ID (3O96), B-Raf V600E Kinase (BRAF V600E) PDB ID (3OG7), Mitogen-Activated Protein Kinase Kinase -1 (MEK-1) PDB ID (3SLS), Extracellular Signal-Regulated Kinases -2 (ERK-2) PDB ID (3I60), Mammalian Target of Rapamycin (mTOR) PDB ID (4JSX), Receptor Tyrosine Kinase (c-Kit) PDB ID (3G0E) and Phosphatidylinositol-3-Kinase (PI3K) PDB ID (4WAF). The following Retrieval of Ligands from PubChem are Nuciferine PubChem CID (10146) and Vemurafenib PubChem CID (42611257). Vemurafenib is used as reference drug. The residues forming the binding pockets, kinase was identified based on extensive literature search.

Table 1: Provides the details of the active site residues used for molecular docking studies for AKT-1, BRAF V600E, MEK-1, ERK-2, mTOR, c-Kit, PI3K proteins

Target protein	Active site residues	Grid size (x y z in A)	Grid center (x y z) coordinates
AKT	ASN54, TRP80, ILE54, SER205, LEU210, THR211, LEU264, LYS268, TYR272, ILE290, ASP292, CYC296	40x40x40	8.373, -6.828, 12.622
BRAF V600E	ILE463, VAL471, LYS483, ALA481, LYS483, LEU505, LEU514, THR529, GLN530, TRP531, CYS532, PHE583, ASP594, PHE595, GLY596	40x28x30	-1.09, -2.28, -20.518
ERK	ARG13, SER27, TYR28, GLU31, GLY32, GLY35, MET36, VAL37, LYS46, VAL49, ALA50, LYS52, ILE54, GLN103, ASP104, MET106, ASP109, LYS112, ASN152, LEU154, ASP165, ARG189, ARG192, TYR231, HIS267, LYS340	40x40x40	7.959, -3.713, 44.557
MTOR	LEU2185, GLU2190, ILE2237, GLY2238, TRP2239, VAL2240, CYS2243, THR2245, MET2345, ILE2356	40x40x40	49.981, -1.370, -47.778
PI3K	TRP780, MET800, LYS802, ASP805, ASP810, TYR836, ILE848, GLU849, VAL850, VAL851, SER854, GLN859, MET922, ILE932, ASP933	40x40x40	-1.612, 9.117, -16.917
MEK	LEU74, ALA76, ASN78, GLY79, LYS97, ILE99, VAL127, ILE141, GLU144, MET146, SER150, GLN153, ASP190, LYS192, SER194, ASN195, ASP208, PHE209, VAL211, SER212	40x40x40	-14.947, 15.367, -28.601
c-KIT	LEU595, VAL603, ALA621, VAL654, THR670, GLU671, TYR672, CYS673, CYS674, GLY676, LEU799, CYS809, ASP810, PHE811	40x40x40	34.165, -3.627, -78.308

From Table 1, Through a thorough examination of the literature, the residues that make up the kinase's binding sites were identified. Based on this evaluation, the pertinent data was collected to pinpoint the crucial atoms that are involved in binding.

In Silico Molecular Docking

A popular docking studies programme called AutoDock Vina can forecast the strength of the interaction between a ligand and a target. Among the most important interactions that AutoDock Vina can foresee throughout the docking process is hydrogen bonding. The programme determines the location and orientation of the hydrogen bond donors and acceptors in the ligand and receptor molecules, using this data to forecast the degree of stability and strength of the hydrogen bonds that will be created between them. The software calculates the distance and orientation of the hydrogen bond donors and acceptors in the ligand and receptor molecules, and this information is used to predict the strength and stability of the hydrogen bonds formed between them.

Table 2: H-Bond distance on multiple molecular targets of melanoma of Nuciferine and Vemurafenib

Target Protein	PDB ID	Nuciferine		Vemurafenib	
		H-Bond Residues	Distances of H-Bonds	H-Bond Residues	Distances of H-Bonds
AKT	3O96	SER205	2.53	THR82	1.83
BRAF V600E	3OG7	CYS532	3.69	CYS532	2.13
ERK	3I60	GLY30	3.35	GLU31	2.13
MTOR	4JSX	VAL2240	3.44	TYR2225	2.74
PI3K	4WAF	LYS802	2.41	VAL851	2.31
MEK	3SLS	ASN78	3.19	GLN153	1.99
c-KIT	3G0E	GLN556	2.89	ASP667	2.25

From Table 2 shows the shortest distances between ligands (Nuciferine and Vemurafenib) and receptors of target proteins. The shortest distance

Table 3: Docking analysis of Nuciferine and Vemurafenib on multiple molecular targets of melanoma

Target	PDB-ID's	Nuciferine			Vemurafenib		
		Kcal/ mol	No. of H-Bond	H-Bonds Binding residues	Kcal/ mol	No. of H-Bond	H-Bonds Binding residues
AKT	3O96	-10.6	2	SER-205, LYS-268	-11.2	1	THR-82
BRAF V600E	3OG7	-9.2	1	CYS-532	-11.4	4	CYS-532, GLN-530, PHE-595, GLY-596
ERK	3I60	-8.8	2	GLY-30, GLN-103	-9.2	3	GLY-30, GLU-31, CYS-164
MTOR	4JSX	-8.5	1	VAL-2240	-9.1	5	GLN-2167, LYS-2187, GLU-2190, ASP-2195, TYR-2225
PI3K	4WAF	-8.3	2	LYS-802, GLU-849	-9.1	3	VAL-850, VAL-851, THR-856
MEK	3SLS	-7.6	2	LEU-74, ASN-78	-8.4	5	GLY-75, ALA-76, SER-150, GLN-153, SER-194
c-KIT	3G0E	-7.2	4	GLU-554, GLN-556, ASP-792, TYR-823	-9.2	3	GLY-676, CYS-673, ASP-677

From this Table 3 shows from RAS-ERK pathway for Nuciferine in BRAF V600E (3OG7) shows highest binding energy (-9.2 Kcal/Mol) and Vemurafenib shows highest binding energy (-11.4 Kcal/Mol) [23]. In PI3K-AKT pathway for Nuciferine in AKT (3O96) shows highest binding energy (-10.6 Kcal/Mol) and Vemurafenib shows highest binding energy (-11.2 Kcal/Mol). Highest number of hydrogen bonds was for Nuciferine was from c-KIT (3G0E) having 4 H-bonds and in Vemurafenib mTOR (4JSX) have 5 H-bonds.

Calculation of Inhibition Constant And Binding Affinity

The expected binding and docking energies are the sum of the intermolecular energy or torsional free energy penalty and the internal energy of the docking ligand, and the inhibition constant (Ki) is calculated in AutoDock4 as follows: Ki = exp(ΔG/RT), where R is the universal gas constant (1.985 × 10−3 kcal mol−1 K−1) and T is the temperature (298.15 K).

Table 4: Inhibition constant of Nuciferine and Vemurafenib on multiple molecular targets of melanoma

Target	PDB ID's	Ki (Inhibition Constant) µm	
		Nuciferine	Vemurafenib
AKT	3O96	166.54	6048.6
BRAF V600E	3OG7	17.73	4309.9
ERK	3I60	34.86	17.736
mTOR	4JSX	57.88	21.001
PI3K	4WAF	81.15	21.001
MEK	3SLS	2.64	68.536
c-KIT	3G0E	5.20	17.736

From Table 4, The highest inhibition constant Ki (Inhibition Constant) for Nuciferine and its Target protein (AKT) having 166.54 µm. In Vemurafenib and its target protein (AKT) having 6048.6 µm.

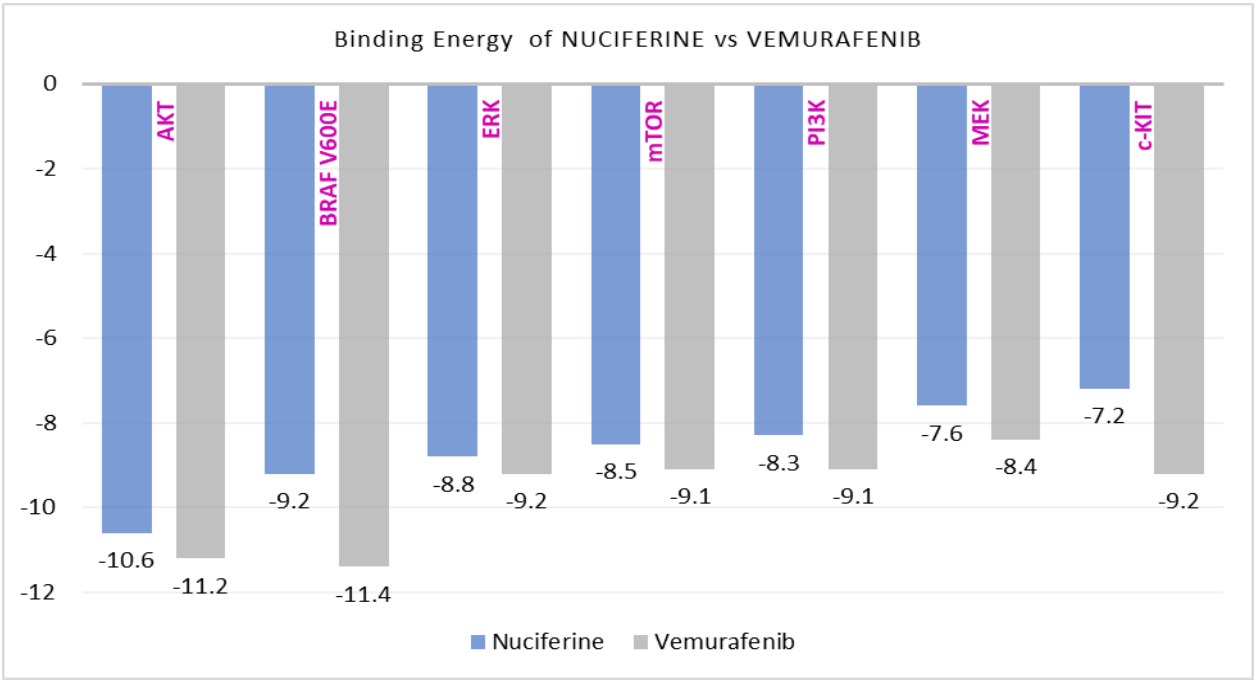

Figure 2: Comparison of binding energy between Nuciferine and Vemurafenib on multiple molecular targets of melanoma plotted as graph.

Pharmacokinetic and Pharmacodynamic Activity Analysis of Nuciferine and Vemurafenib

Pharmacokinetic analysis identifies key factors that are helpful in the advancement and discovery of novel drugs by using SwissADME. The PASS relies heavily on the idea of the pharmacological biological activity spectrum, which also serves as the foundation for forecasting a variety of biological activity types for various chemicals (Poroikov *et al.,* 2003). The PASS predictions are able to be utilized and evaluated in a variety of ways. For something like a specific chemical, Pa ratings near 1 and Pi value system near 0 are indicative of the drug's most likely actions. Using the PreADMET web service, Nuciferine and Vemurafenib's ADMET silhouettes were anticipated (https://preadmet.webservice.bmdrc.org/).

Table 5: Prediction of ADME by SwissADME (absorption and distribution):

Molecule	Swiss ADME								
	Absorption	Distribution							
	GI absorption	BBB permeant	P-gp substrate	CYP1A2 inhibitor	CYP2C19 inhibitor	CYP2C9 inhibitor	CYP2D6 inhibitor	CYP3A4 inhibitor	Log Kp (skin permeation)
Nuciferine	High	Yes	Yes	No	No	No	Yes	Yes	-5.67 cm/s
Vemurafenib	Low	No	No	No	Yes	Yes	No	Yes	-5.76 cm/s

From Table 5, The ability of a drug to cross the Blood-Brain Barrier (BBB) and act on the central nervous system (CNS) is a crucial factor in determining its effectiveness for treating neurological disorders. Therefore, a drug that is BBB permeant can be beneficial in some cases. Log Kp is a measure of the permeability of a compound across the skin. Log Kp provides information on the compound's ability to penetrate the skin barrier. A higher Log Kp value indicates that the compound is more lipophilic and has a greater potential to permeate the skin. GI absorption refers to the process by which drugs or other substances are absorbed from the gastrointestinal (GI) tract into the bloodstream. Absorption can occur through various mechanisms such as passive diffusion, active transport, and facilitated diffusion.

Table 6: Prediction of ADME by SwissADME (physiochemical properties and druglikeness):

Compounds	PubChem ID	Molecular Mass (Da)	Hydrogen bond donor (HBD <5)	Hydrogen bond acceptor (HBA <10)	Log P < 5	Molar refractivity (40–130)	Drug likeness >0
Nuciferine	10146	295.38	0	3	3.27	91.96	0.55
Vemurafenib	42611257	489.92	2	6	4.84	124.21	0.55

From Table 6, Druglikeness is a term used to describe the likelihood that a molecule will be developed into a drug. It refers to the set of physicochemical and structural properties that are commonly found in compounds that have good pharmacokinetic and pharmacodynamic properties, which are necessary for successful drug development. Druglikeness can be evaluated using various criteria, such as Lipinski's rule of five, which evaluates the molecule's molecular weight, lipophilicity, number of hydrogen bond donors and acceptors, and other properties. Other druglikeness criteria may include the presence of certain functional groups, a specific stereochemistry, and a low toxicity profile.

Table 7: Prediction of ADME by PreADMET:

Molecule	PreADMET				
	Absorption			Distribution	
	%HIA	Caco-2 (nm/sec)	MDCK (nm/sec)	Plasma Protein Binding%	BBB (cbrain/cblood)
Nuciferine	100	57.5747	226.456	74.454071	1.65054
Vemurafenib	94.294819	3.31445	0.0581486	95.663756	1.35427

From Table 7, Plasma protein binding refers to the extent to which drugs or other substances bind to proteins in the blood plasma. When a drug is introduced into the bloodstream, it can bind to plasma proteins, which can affect its distribution, metabolism, and elimination from the body. MDCK stands for Madin-Darby Canine Kidney, which is a cell line commonly used in vitro as a model for studying drug absorption, metabolism, and toxicity. MDCK cells are commonly used in drug discovery and development to assess drug permeability across cell membranes and predict oral bioavailability. In vitro studies using MDCK cells can provide valuable information about the absorption and metabolism of potential drug candidates, which can help guide the selection of compounds for further development. HIA stands for human intestinal absorption, which refers to the extent to which a drug or other substance is absorbed from the gastrointestinal tract into the systemic circulation in humans. The HIA value is an important pharmacokinetic parameter used in drug development to evaluate the oral bioavailability and efficacy of a drug candidate.

Table 8: Biological activity prediction of the compounds using the PASS server:

Molecule	Pa	Pi	Activity prediction
Nuciferine	0.936	0.004	5 Hydroxytryptamine release stimulant
	0.852	0.009	Antineurotic
	0.836	0.003	Antitussive
	0.787	0.001	Dopamine D2A antagonist
	0.767	0.003	Histamine release stimulant
	0.751	0.004	Oxygen scavenger
	0.724	0.005	MAP kinase stimulant
Vemurafenib	0.912	0.000	JNK mitogen-activated protein kinase inhibitor
	0.882	0.002	Growth factor agonist
	0.826	0.002	Stem cell growth factor agonist
	0.813	0.003	Raf kinase inhibitor
	0.458	0.021	Protein kinase inhibitor
	0.462	0.083	Antineoplastic
	0.218	0.016	MAP kinase inhibitor
	0.163	0.070	Tyrosine kinase inhibitor

From Table 9, The PASS internet server was used to predict the Pa and Pi values of Nuciferine and Vemurafenib. Pa refers probability to be active to and Pi refers to probability to be inactive.

2D and 3d Interactions of Docked Complexes

Biovia Discovery Studio is a powerful software suite for molecular modeling that includes tools for visualizing and analyzing 2D and 3D interactions between molecules [24]. The software allows users to interactively explore and manipulate molecular structures to identify and visualize 2D interactions, such as hydrogen bonds, hydrophobic bonds, electrostatic interactions, and Pi-Pi stacked interactions. This information can then be used to better understand the behavior of molecules and to guide the design of new compounds with desired properties.

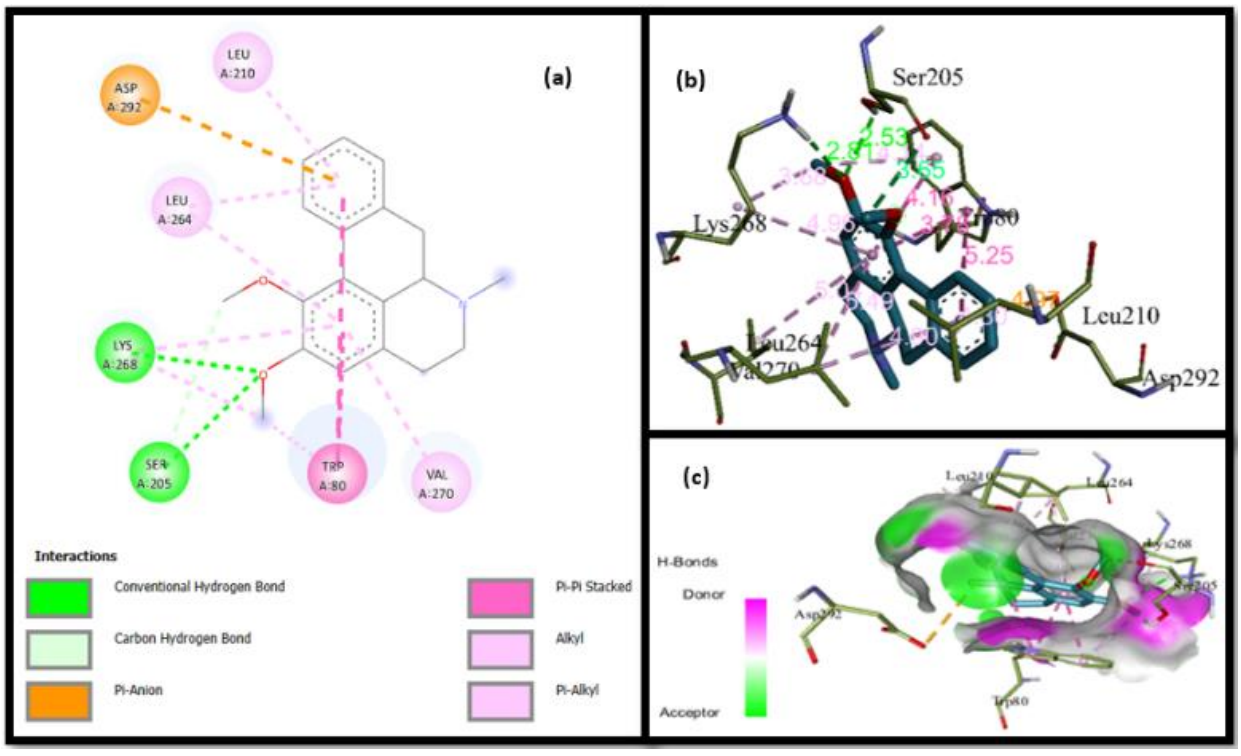

Figure 3: 2D interaction of [3O96] AKT and Nuciferine (a). 3D interaction of [3O96] AKT and Nuciferine (b). H-bonds interaction of [3O96] AKT and Nuciferine graphical representation (c).

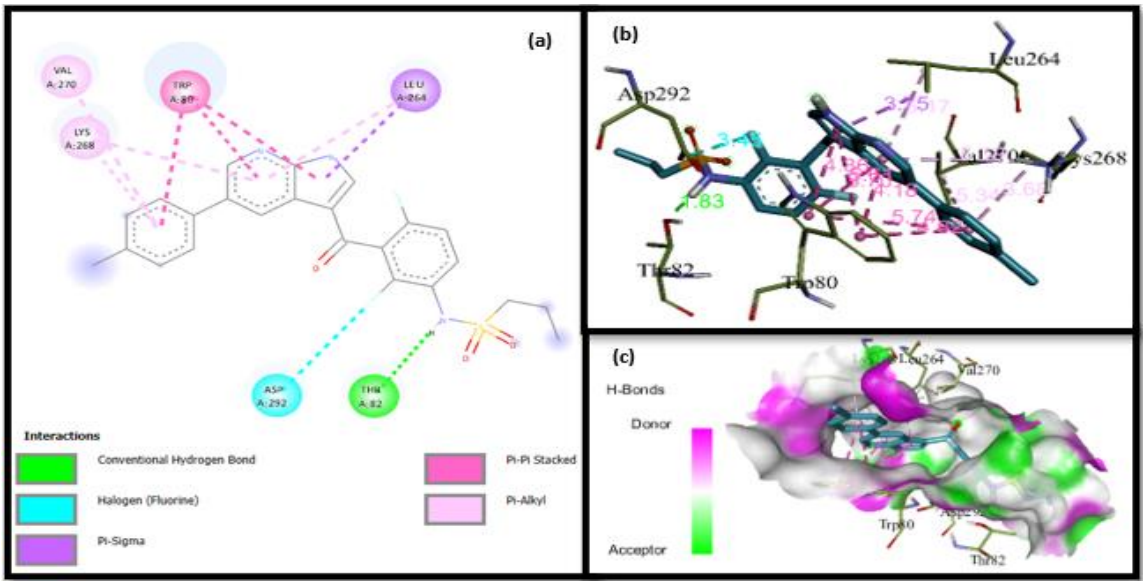

Figure 4: 2D interaction of [3O96] AKT and Vemurafenib(a). 3D interaction of [3O96] AKT and Vemurafenib (b). H-bonds interaction of [3O96] AKT and Vemurafenib graphical representation (c).

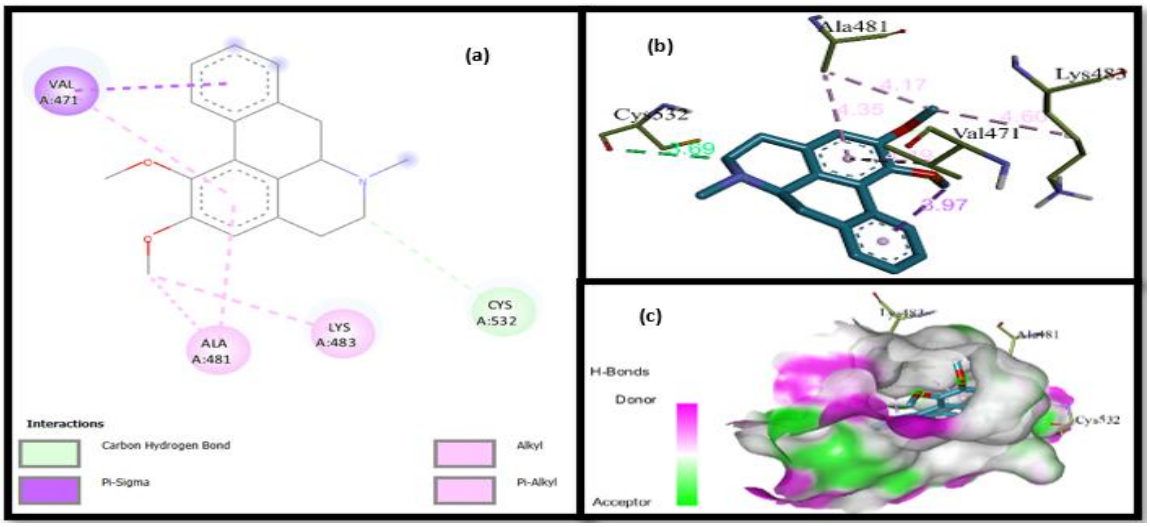

Figure 5: 2D interaction of [3OG7] BRAF V600E and Nuciferine (a). 3D interaction of [3OG7] BRAF V600E and Nuciferine (b). H-bonds interaction of [3OG7] BRAF V600E and Nuciferine graphical representation (c).

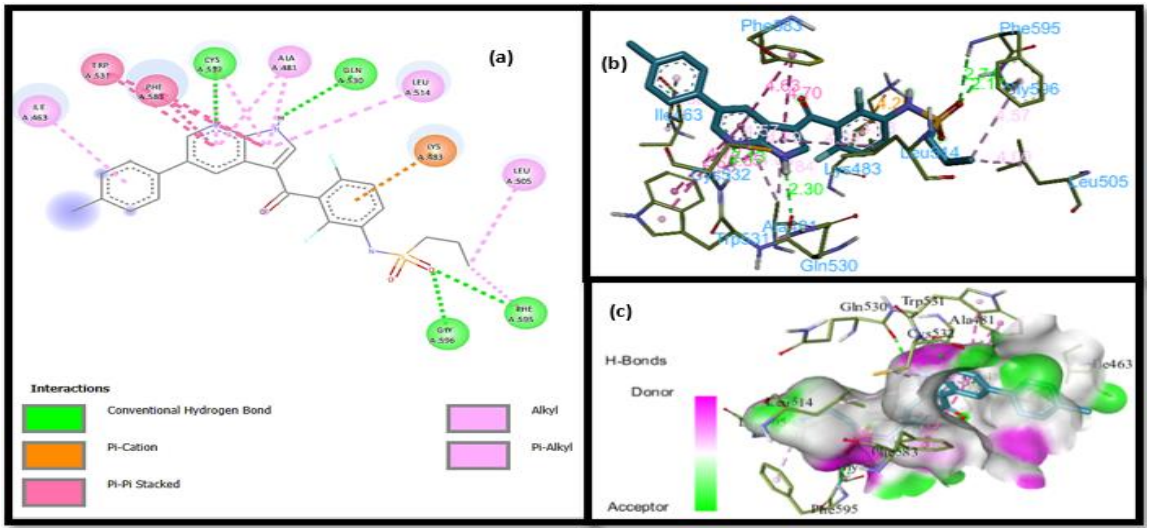

Figure 6: 2D interaction of [3OG7] BRAF V600E and Vemurafenib(a). 3D interaction of [3OG7] BRAF V600E and Vemurafenib (b). H-bonds interaction of [3OG7] BRAF V600E and Vemurafenib graphical representation (c).

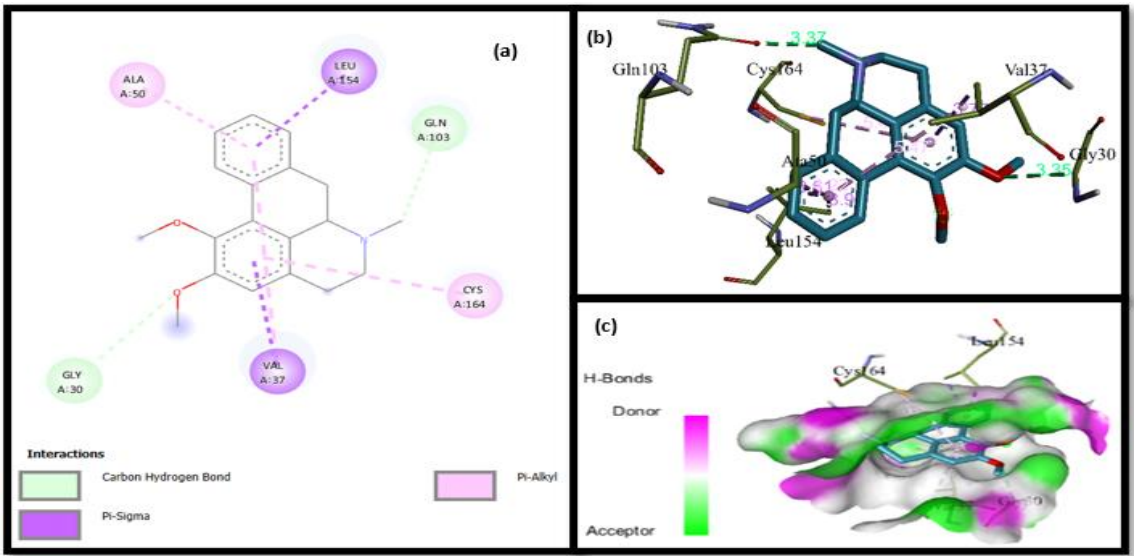

Figure 7: 2D interaction of [3I60] ERK and Nuciferine (a). 3D interaction of [3I60] ERK and Nuciferine (b). H-bonds interaction of [3I60] ERK and Nuciferine graphical representation (c).

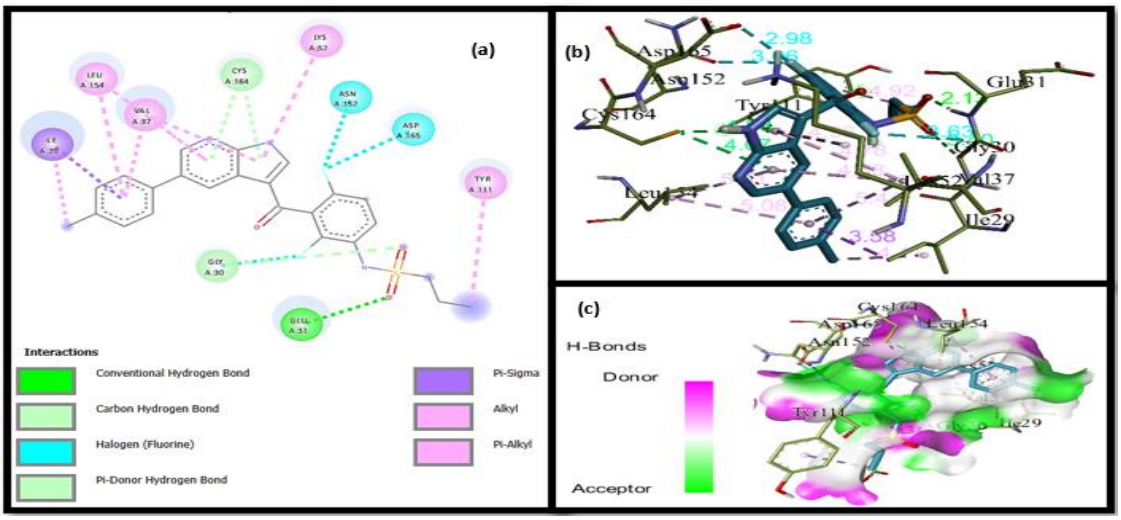

Figure 8: 2D interaction of [3I60] ERK and Vemurafenib(a). 3D interaction of [3I60] ERK and Vemurafenib (b). H-bonds interaction of [3I60] ERK and Vemurafenib graphical representation (c).

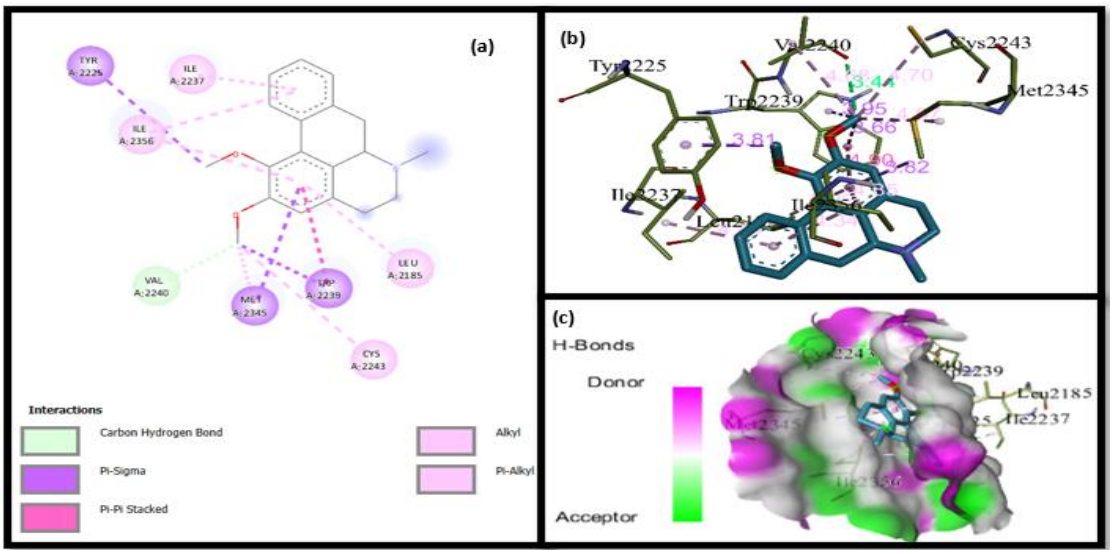

Figure 9: 2D interaction of [4JSX] mTOR and Nuciferine (a). 3D interaction of [4JSX] mTOR and Nuciferine (b). H-bonds interaction of [4JSX] mTOR and Nuciferine graphical representation (c).

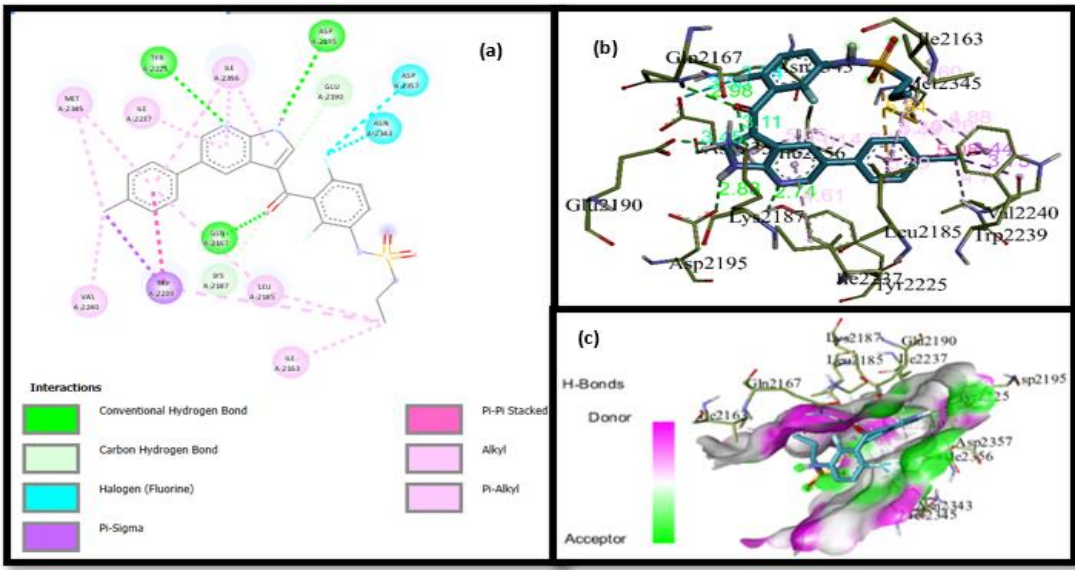

Figure 10: 2D interaction of [4JSX] mTOR and Vemurafenib(a). 3D interaction of [4JSX] mTOR and Vemurafenib (b). H-bonds interaction of [4JSX] mTOR and Vemurafenib graphical representation (c).

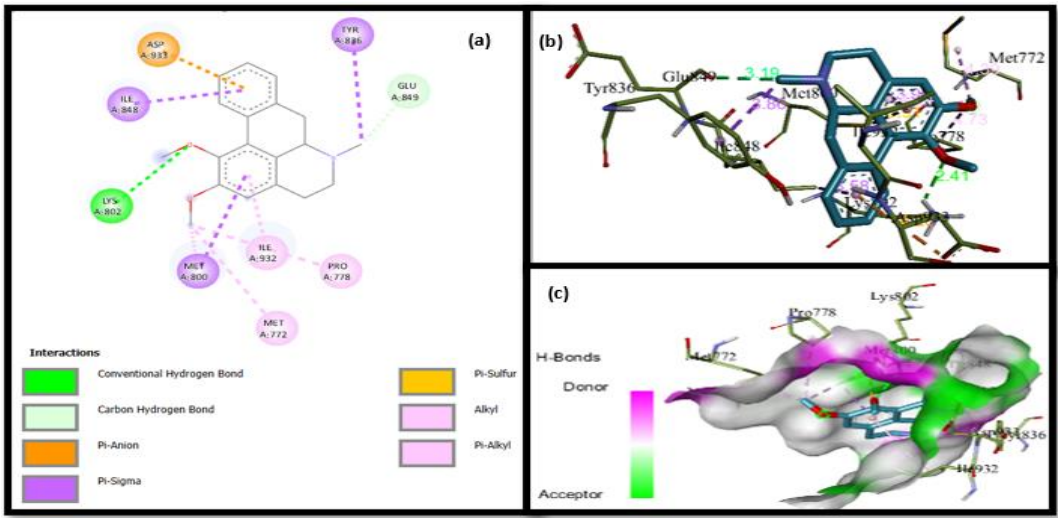

Figure 11: 2D interaction of [4WAF] PI3K and Nuciferine (a). 3D interaction of [4WAF] PI3K and Nuciferine (b). H-bonds interaction of [4WAF] PI3K and Nuciferine graphical representation (c).

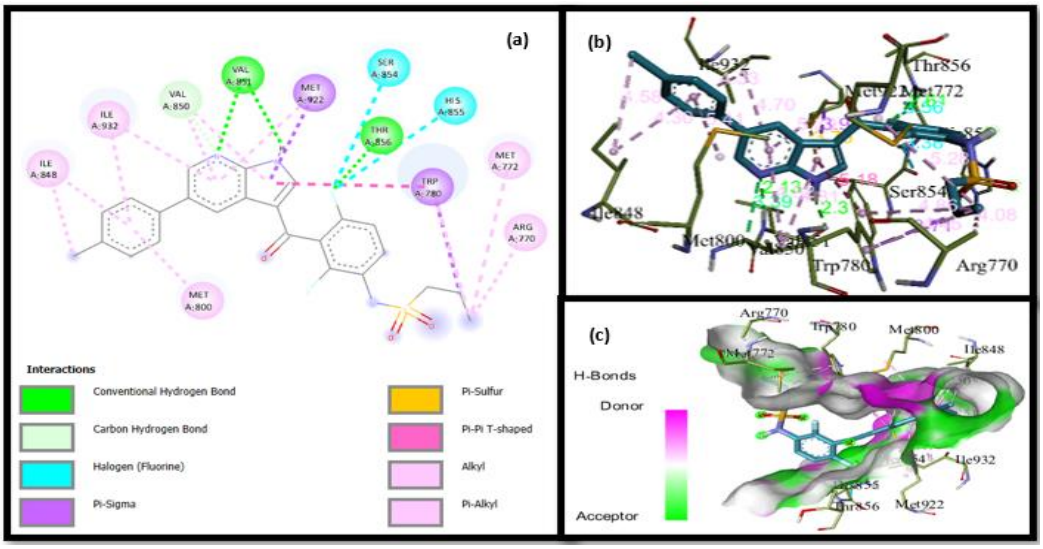

Figure 12: 2D interaction of [4WAF] PI3K and Vemurafenib(a). 3D interaction of [4WAF] PI3K and Vemurafenib (b). H-bonds interaction of [4WAF] PI3K and Vemurafenib graphical representation (c).

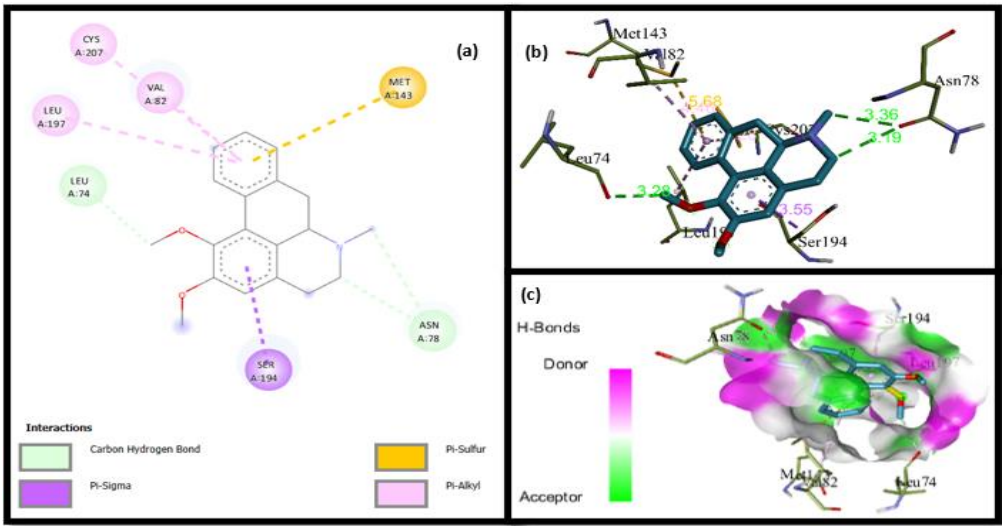

Figure 13: 2D interaction of [3SLS] MEK and Nuciferine (a). 3D interaction of [3SLS] MEK and Nuciferine (b). H-bonds interaction of [3SLS] MEK and Nuciferine graphical representation (c).

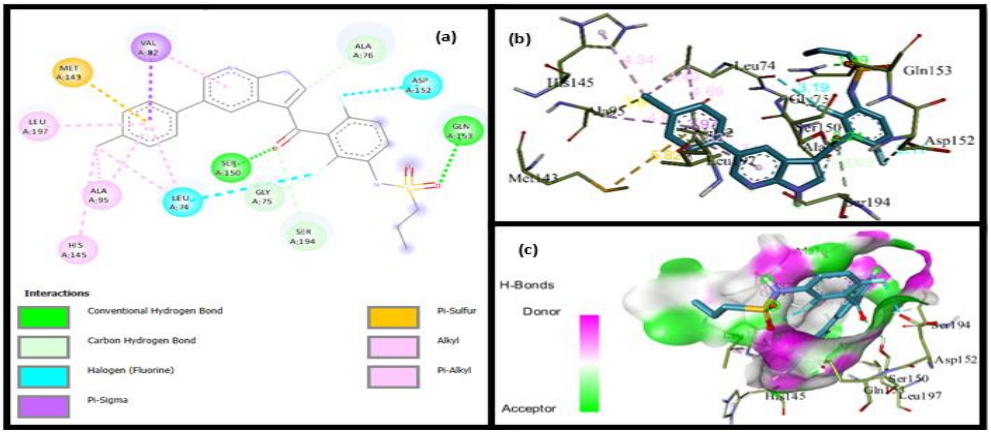

Figure 14: 2D interaction of [3SLS] MEK and Vemurafenib(a). 3D interaction of [3SLS] MEK and Vemurafenib (b). H-bonds interaction of [3SLS] MEK and Vemurafenib graphical representation (c).

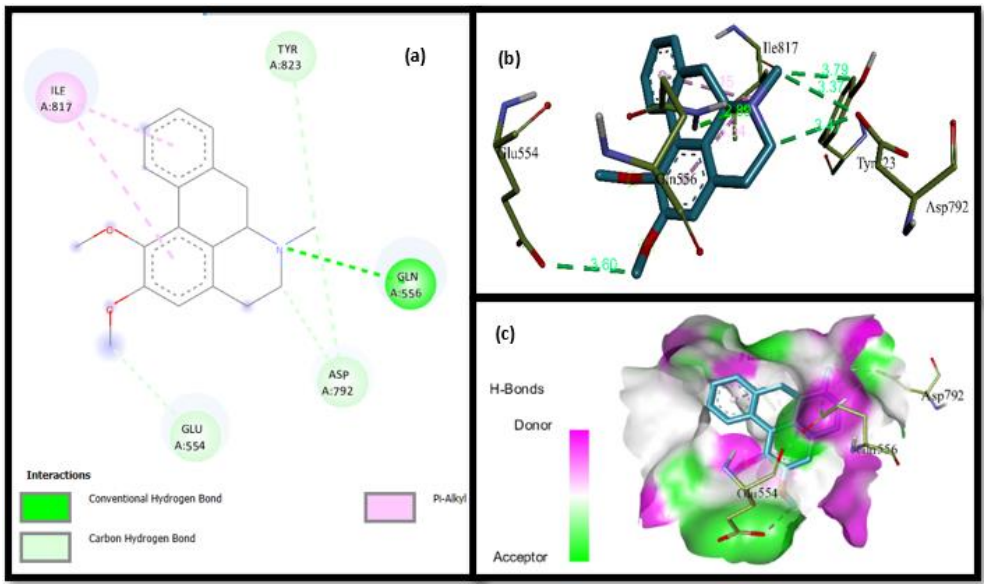

Figure 15: 2D interaction of [3G0E] c-KIT and Nuciferine (a). 3D interaction of [3G0E] c-KIT and Nuciferine (b). H-bonds interaction of [3G0E] c-KIT and Nuciferine graphical representation (c).

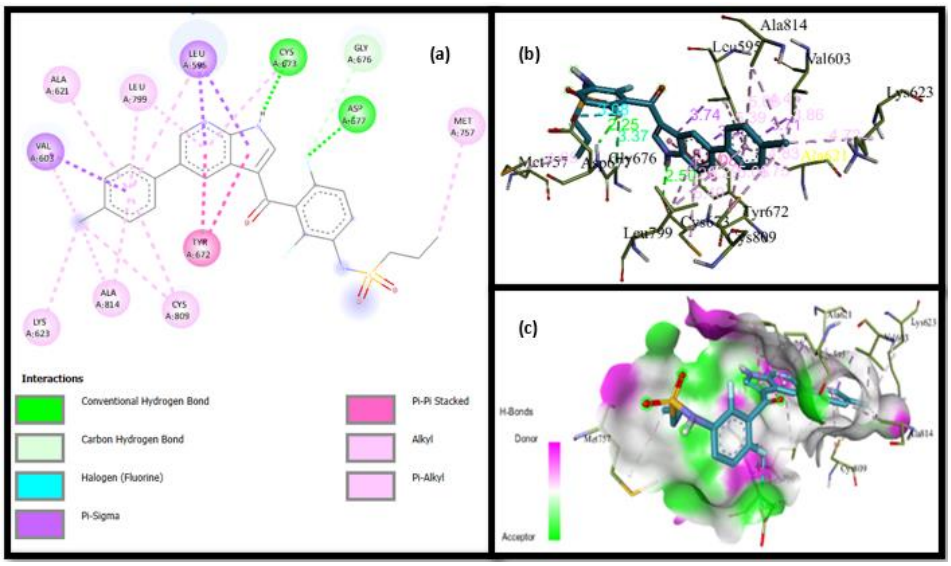

Figure 16: 2D interaction of [3G0E] c-KIT and Vemurafenib(a). 3D interaction of [3G0E] c-KIT and Vemurafenib (b). H-bonds interaction of [3G0E] c-KIT and Vemurafenib graphical representation (c).

In the molecular studies, BIOVIA Discovery Studio Visualizer was used for docking structure visualized (2D interactions, 3D interactions and H-Bond interactions) to viewing all the fourteen docking structures of [3O96] AKT and nuciferine (figure 3), [3O96] AKT and vemurafenib (figure 4) [25], [3OG7] BRAF V600E and nuciferine (figure 5), [3OG7] BRAF V600E and Vemurafenib (figure 6) [26], [3I60] ERK and Nuciferine (figure 7), [3I60] ERK and Vemurafenib (figure 8) [27], [4JSX] mTOR and Nuciferine (figure 9), [4JSX] mTOR and Vemurafenib (figure 10) [28], [4WAF] PI3K and nuciferine (figure 11), [4WAF] PI3K and Vemurafenib (figure 12) [29], [3SLS] MEK and Nuciferine (figure 13), [3SLS] MEK and Vemurafenib (figure 14) [30], [3G0E] c-KIT and Nuciferine (figure 15) and [3G0E] c-KIT and Vemurafenib (figure 16).

Highest docking energy for Nuciferine [ΔG (kcal/mol)] in RAS-ERK pathway is [3OG7] BRAF V600E [-9.2 kcal/mol] (table 4). In PI3K/AKT pathway Highest docking energy [ΔG (kcal/mol)] for Nuciferine is [3O96] AKT [-10.6 kcal/mol] (table 4). Hence Nuciferine also shows best result that obstructs melanoma and it have best result for antiproliferation also. It stops in both the pathways to go for further downstream for proliferation and melanoma.

CONCLUSION

In silico studies shows that Nuciferine can stop both RAS-ERK and PI3K/AKT pathway for melanoma. It shows that Nuciferine have anti-proliferative potentials. Lipinski shows positive and shows 0 violations in both Nuciferine and Vemurafenib. Hence it is safe to use. From the observation Nuciferine in BRAF V600E (3OG7) shows highest binding energy (-9.2 Kcal/Mol) and Vemurafenib shows highest binding energy (-11.4 Kcal/Mol). In PI3K-AKT pathway for Nuciferine in AKT (3O96) shows highest binding energy (-10.6 Kcal/Mol) and Vemurafenib shows highest binding energy (-11.2 Kcal/Mol).

Author Contribution

Iswaryalakshmi Saravanabavan carried out experiments of this research like, *in silico* studies docking, ADMET studies - Abiraamasundari Ramapalaniappan; and contributed to writing, experimentation, result reporting and original draft preparation. Veerabhuvaneshwari Veerichetty participated in the analysis of Nuciferine and Vemurafenib computational analysis in Skin Melanoma cells and conceptualization, methodology planning, research supervision and data analysis of results and manuscript preparation.

Acknowledgement

The authors are thankful for the support provided by Department of Bio-Technology, Kumaraguru College of Technology, Coimbatore (TN), India and [2]SpinoS Life science and Research Private Limited.

Funding: This research received no external funding.

Conflicts of Interest

The authors declare no conflict of interest.

ORCID ID

Veerabhuvaneshwari Veerichetty: http://orcid.org/0000-0002-5617-0354
Iswaryalakshmi Saravanabavan: http://orcid.org/0009-0000-8718-2705
Abiraamasundari Ramapalaniappan: http://orcid.org/0000-0002-3103-1462

REFERENCES

1. Lin K, Baritaki S, Militello L, Malaponte G, Bevelacqua Y, Bonavida B. The Role of B-RAF Mutations in Melanoma and the Induction of EMT via Dysregulation of the NF-κB/Snail/RKIP/PTEN Circuit. Genes & cancer. 2010;1(5):409-20.
2. Pritchard AL, Hayward NK. Molecular pathways: mitogen-activated protein kinase pathway mutations and drug resistance. Clinical cancer research. 2013;19(9):2301-9.
3. Peng Y, Wang Y, Zhou C, Mei W, Zeng C. PI3K/Akt/mTOR pathway and its role in cancer therapeutics: are we making headway?. Frontiers in oncology. 2022;12:819128.
4. Maner BS, Dupuis L, Su A, Jueng JJ, Harding TP, Meisenheimer J, Siddiqui FS, Hardack MR, Aneja S, Solomon JA. Overview of

genetic signaling pathway interactions within cutaneous malignancies. J. Cancer Metastasis Treat. 2020;6:37-9.
5. Wu WI, Voegtli WC, Sturgis HL, Dizon FP, Vigers GP, Brandhuber BJ. Crystal structure of human AKT1 with an allosteric inhibitor reveals a new mode of kinase inhibition. PloS one, 2010;5(9):e12913.
6. Bollag G, Hirth P, Tsai J, Zhang J, Ibrahim PN, Cho H, Nolop K. Clinical efficacy of a RAF inhibitor needs broad target blockade in BRAF-mutant melanoma. Nature 2010;467(7315):596-599.
7. Aronov AM, Tang Q, Martinez-Botella G, Bemis GW, Cao J, Chen G, Xie X. Structure-guided design of potent and selective pyrimidylpyrrole inhibitors of extracellular signal-regulated kinase (ERK) using conformational control. Journal of medicinal chemistry, 2009;52(20):6362-6368.
8. Yang H, Rudge DG, Koos JD, Vaidialingam B, Yang HJ, Pavletich NP. mTOR kinase structure, mechanism and regulation. Nature 2013;*497*(7448):217-223.
9. Barsanti PA, Aversa RJ, Jin X, Pan Y, Lu Y, Elling R, Yue Q. Structure-based drug design of novel potent and selective tetrahydropyrazolo [1, 5-a] pyrazines as ATR inhibitors. ACS Medicinal Chemistry Letters, 2015;*6*(1):37-41.
10. Meier C, Brookings DC, Ceska TA, Doyle C, Gong H, McMilla D, Allen RA. Engineering human MEK-1 for structural studies: A case study of combinatorial domain hunting. Journal of structural biology 2012;177(2):329-334.
11. Gajiwala KS, Wu JC, Christensen J, Deshmukh GD, Diehl W, DiNitto JP, Demetri GD. KIT kinase mutants show unique mechanisms of drug resistance to imatinib and sunitinib in gastrointestinal stromal tumor patients. Proceedings of the national Academy of sciences. 2009;106(5):1542-1547.
12. Rose PW, Prlić A, Altunkaya A, Bi C, Bradley AR, Christie CH, Burley SK. The RCSB protein data bank: integrative view of protein, gene and 3D structural information. Nucleic acids research, gkw1000, 2016.
13. National Center for Biotechnology Information PubChem Compound Summary for CID 10146, Nuciferine. 2023. Retrieved March 28, 2023 from https://pubchem.ncbi.nlm.nih.gov/compound/Nuciferine.
14. National Center for Biotechnology Information PubChem Compound Summary for CID 42611257, Vemurafenib. 2023. Retrieved March 28, 2023 from https://pubchem.ncbi.nlm.nih.gov/compound/Vemurafenib.
15. Filimonov DA, Lagunin AA, Gloriozova TA, Rudik AV, Druzhilovskii DS, Pogodin PV, Poroikov VV. Prediction of the biological activity spectra of organic compounds using the PASS online web resource. Chemistry of Heterocyclic Compounds. 2014;50:444-457.
16. Daina A, Michielin O, Zoete V. SwissADME: a free web tool to evaluate pharmacokinetics, drug-likeness and medicinal chemistry friendliness of small molecules. Scientific reports. 2017;7(1):42717.
17. Lee SK, Chang GS, Lee IH, Chung JE, Sung KY, No KT. The PreADME: pc-based program for batch prediction of adme properties. EuroQSAR, 2004;9:5-10.
18. Lee SK, Lee IH, Kim HJ, Chang GS, Chung JE, No KT. The PreADME Approach: Web-based program for rapid prediction of physico-chemical, drug absorption and drug-like properties. EuroQSAR 2002 Designing Drugs and Crop Protectants: processes, problems and solutions, 2003, 418-420
19. Eberhardt J, Santos-Martins D, Tillack AF, Forli S. AutoDock Vina 1.2. 0: New docking methods, expanded force field, and python bindings. Journal of chemical information and modeling, 2021;61(8):3891-3898.
20. Trott O, Olson AJ. AutoDock Vina: improving the speed and accuracy of docking with a new scoring function, efficient optimization, and multithreading. Journal of computational chemistry, 2010;31(2):455-461.
21. Ortiz CL, Completo GC, Nacario RC, Nellas RB. Potential inhibitors of galactofuranosyltransferase 2 (GlfT2): molecular docking, 3D-QSAR, and in silico ADMETox studies. Scientific reports. 2019;9(1):17096.
22. Wang GM, Wang X, Zhu JM, Guo BB, Yang Z, Xu ZJ, Li B, Wang HY, Meng LH, Zhu WL, Ding J. Docking-based structural splicing and reassembly strategy to develop novel deazapurine derivatives as potent B-RafV600E inhibitors. Acta pharmacologica sinica. 2017;38(7):1059-68.
23. Umar BA, Uzairu A, Shallangwa GA, Uba S. Rational drug design of potent V600E-BRAF kinase inhibitors through molecular docking simulation. The Journal of Engineering and Exact Sciences. 2019;5(5):0469-81.
24. Design LIGAND. Pharmacophore and ligand-based design with Biovia Discovery Studio®. BIOVIA. California. 2014.
25. Hwang SY, Chae JI, Kwak AW, Lee MH, Shim JH. Alternative options for skin cancer therapy via regulation of AKT and related signaling pathways. International Journal of Molecular Sciences. 2020;21(18):6869.
26. Hassan SS, Abbas SQ, Ali F, Ishaq M, Bano I, Hassan M, Jin HZ, Bungau SG. A Comprehensive *in silico* exploration of pharmacological properties, bioactivities, molecular docking, and anticancer potential of vieloplain F from Xylopia vielana Targeting B-Raf Kinase. Molecules. 2022;27(3):917.
27. Goetz EM, Ghandi M, Treacy DJ, Wagle N, Garraway LA. ERK mutations confer resistance to mitogen-activated protein kinase pathway inhibitors. Cancer research. 2014;74(23):7079-89.
28. Xie C, Chen X, Zheng M, Liu X, Wang H, Lou L. Pharmacologic characterization of SHR8443, a novel dual inhibitor of phosphatidylinositol 3-kinase and mammalian target of rapamycin. Oncotarget. 2017;8(64):107977.
29. Vollono L, Falconi M, Gaziano R, Iacovelli F, Dika E, Terracciano C, Bianchi L, Campione E. Potential of curcumin in skin disorders. Nutrients. 2019;11(9):2169.
30. Nawrot-Hadzik I, Choromańska A, Abel R, Preissner R, Saczko J, Matkowski A, Hadzik J. Cytotoxic effect of vanicosides A and B from Reynoutria sachalinensis against melanotic and amelanotic melanoma cell lines and in silico evaluation for inhibition of BRAFV600E and MEK1. International Journal of Molecular Sciences. 2020;21(13):4611.

HOW TO CITE THIS ARTICLE
Veerichetty V, Saravanabavan I, Ramapalaniappan A. *In silico* kinase inhibition profiling of BRAF and AKT Signaling in Melanoma Cells with Nuciferine. J Phytopharmacol 2023; 12(3):152-163. doi: 10.31254/phyto.2023.12303